



Voltammetric determination of the antimalarial drug chloroquine using a glassy carbon electrode modified with reduced graphene oxide on WS₂ quantum dots

Monika Srivastava¹ · Preeti Tiwari¹ · Vineet Kumar Mall¹ · S. K. Srivastava² · Rajiv Prakash¹

Received: 10 February 2019 / Accepted: 19 May 2019 / Published online: 11 June 2019
© Springer-Verlag GmbH Austria, part of Springer Nature 2019

Abstract

A voltammetric method is described for the determination of chloroquine (CQ) and validated simultaneously by two techniques and in three different conditions. The WS₂ quantum dots (WS₂ QDs) were synthesized by a hydrothermal method and then placed on reduced graphene oxide (rGO) sheets. The resulting composite material was then deposited on a glassy carbon electrode (GCE) where it showed excellent electroactivity. The modified GCE responds to chloroquine at a typical potential maximum of 1.2 V (vs. AgCl/Ag). Techniques including cyclic voltammetry and differential pulse voltammetry were tested. Features of merit include (a) a wide linear response (in the 0.5 μM to 82 μM CQ concentration range), (b) an electrochemical sensitivity of 0.143–0.90 μA·μM⁻¹·cm⁻², and a 40–120 nM limit of detection (at S/N = 3). The sensor has excellent selectivity even in the presence of potentially interfering biological compounds. Responses were tested in phosphate buffer, human serum and pharmaceutical formulations, and no cross reactivity or matrix effects were found. In all the three cases, quite satisfactory recoveries were obtained.

Keywords Chloroquine phosphate · Anti-malarial drug · Reduced graphene oxide · WS₂ quantum dots · Synergistic effect

Introduction

Chloroquine (CQ) is extensively used in the treatment of sudden attacks of malaria and elimination of porphyria for many decades. This drug is widely used for curing rheumatoid arthritis and similar kinds of collagen diseases. Chloroquine is also used for amoebic hepatitis treatment [1–3]. Various strains of *Plasmodium falciparum* have developed resistance against CQ [4]. But due to its low cost this drug is still widely used in developing countries. It is

also recommended as a strong anti-cancerous agent [5, 6]. High doses of this drug may cause several side effects like heart attack [7]. There are various analytical methods reported in the literature to monitor the concentration of drug like spectrophotometric method [8], high performance liquid chromatography with fluorescence detection [9, 10], chemiluminescence including radiostorage- and photostorage-chemiluminescence (CL) [11] and voltammetric methods [12]. Among all methods voltammetric methods got immense attention due to its fast response, less volume consumption of samples, high selectivity and sensitivity.

Graphene is an atom-thick two dimensional crystalline carbon film with sp² hybrid carbon atoms. It reveals the unprecedented amalgamation of beneficial properties such as remarkable mechanical strength, large surface area, high thermal conductivity and extraordinary electrical properties like tremendous charge carrier mobility and conductivity [13, 14]. Due to these peculiar material properties, graphene have grabbed significant attention and proved their applicability in the fields of sensors [15, 16], catalysis [17], energy-storage [18], electronics [19] and optoelectronics [20]. The graphene oxide (GO) possesses various hydrophilic groups like hydroxyl carboxyl, and epoxy and

Electronic supplementary material The online version of this article (<https://doi.org/10.1007/s00604-019-3525-3>) contains supplementary material, which is available to authorized users.

✉ Monika Srivastava
monikabh.srivastava@gmail.com

✉ Rajiv Prakash
rprakash.mst@iitbhu.ac.in

¹ School of Materials Science and Technology, Indian Institute of Technology, Banaras Hindu University, Varanasi 221005, India

² Department of Physics, Institute of Science, Banaras Hindu University, Varanasi 221005, India

also renders the possibility of functionalization using covalent or non-covalent bindings. These functional groups also allow dispersion of GO in aqueous solution [21]. Further, the conductivity of GO is found to be lesser than that of reduced graphene oxide (rGO). So, in place of GO, rGO can also be used wherever applicable [22, 23]. Utilizing the beneficial film like structure, graphene based composites by incorporation of graphene with diverse functional nanomaterials like metal compounds [24], noble metals [25], carbonaceous materials [26], polymeric materials [27] etc. have been prepared which showed enhanced mechanical, electrical, chemical, mechanical and catalytic properties. Consequently, varieties of sensors have been developed in the recent scenario depicting great stability, sensitivity and selectivity [28–33].

Apart from graphene, two dimensional analogues like transition metal dichalcogenides have also been gaining attention because of similar properties as that of graphene. 2D tungsten disulfide (WS_2) nanosheet is one of the members of this family. It has 2D building blocks of S-W-S layers which are weakly bound by Vander Waals forces. Because of the exclusive chemical, electronic and mechanical properties, it has been used in several fields [34–36]. However, if the size of WS_2 is controlled, zero dimensional WS_2 quantum dots can be synthesized with size in the range of 1–10 nm. Not many reports have been published on the synthesis and applications of WS_2 QDs [37]. In comparison to the nanosheets, quantum dots possess larger surface area and rich exposed edges which is benign to the electrocatalytic activity towards electrochemical sensing. Also, due to the luminescent properties of the dots, they have been used in the fields of sensing, bioimaging, catalysis, electronics, hydrogen evolution reaction etc. [38, 39]. Coating of QDs over 2D materials can help to prevent the aggregation and enhance the stability of these materials. The WS_2 QDs decorated rGO sheets can act as immensely active electrocatalyst to enhance electrode kinetics.

The paper describes fabrication, characterization and analytical performance of a chloroquine sensor based on the rGO@ WS_2 QDs modified glassy carbon electrode by simple voltammetric techniques in phosphate buffer at pH 6. WS_2 QDs is synthesized hydrothermally and GO was synthesized by modified Hummer's method followed by reduction. Proposed sensor is highly reproducible, stable and sensitive for the determination of CQ in broad concentration range of 0.5 μM –82.4 μM .

Experimental section

Materials

Chloroquine phosphate was brought from Sigma, Aldrich, USA. Absolute ethanol, Na_2HPO_4 , NaH_2PO_4 and distilled water were purchased from Merck, India. For electro-sensing of Chloroquine phosphate freshly prepared solution

was prepared using deionised water (DI). $Na_2WO_4 \cdot 2H_2O$ was brought from SRL private Ltd. L-cysteine was procured from Merck, India. Conc. H_2SO_4 , Conc. HCl, Conc. H_3PO_4 , distilled water and Conc. H_2O_2 were purchased from Merck, India. All other chemicals like Hydrazine hydrate, graphite powder and $KMnO_4$ were of analytical grade and used as such with no additional purification. Blood samples (from Volunteers) for the analysis of Chloroquine in real sample was collected from hospital, IMS, BHU, Varanasi, India.

Instrumentation

The entire electrochemical experiments were executed using Autolab (PGSTAT, 302, The Netherlands). Three electrode assembly was used for electrochemical studies. Glassy carbon electrode (GCE) was employed as a working electrode, Pt disc electrode was used as counter electrode, Ag/AgCl is applied as reference electrode.

UV-Vis. spectra were recorded with a spectrophotometer, Epoch 2 microplate reader Biotech, USA in quartz cuvette having 1 cm optical path length. Transmission electron microscopy images were obtained by using TECHNAI G2 20 TWIN (Czech Republic) run at an accelerating voltage of 200 keV on copper grid coated with carbon. Confirmation of the different functional groups present in rGO@ WS_2 QDs were done by FT-IR measurements using Nicolet 380 FT-IR spectrometer in the transmission mode (Thermo Nicolet Corporation, USA), which was equipped with a beam splitter and DTGS KBr detector.

Preparation of WS_2 QDs

WS_2 QDs were synthesized through hydrothermal method in a single step. Sodium tungstate dihydrate ($Na_2WO_4 \cdot 2H_2O$) (0.25 g) and L-cysteine ($HO_2CCH(NH_2)CH_2SH$) (0.5 g) (1:2 w/w) were mixed in DI water separately and both the solutions were constantly stirred for 10–15 min. Further the two solutions were uniformly mixed, again followed by continuous stirring for 15 min and temperature was maintained at 40 °C. In the next step, 12 N concentrated HCl was added in required amount to set pH at 3.0. To initiate hydrothermal process, the above mixture was poured into stainless steel lined Teflon autoclave of 100 mL capacity. Initially temperature was set at 120 °C for 2–3 h and further 190 °C for 46 h. Then reaction mixture was left in the autoclave for attaining room temperature. Finally yellow colloidal solution of WS_2 was obtained which was poured into dialysis bag of retained molecular weight 2000 Da. Then the dialyzed bag was left in ideal condition for 3–4 days to get WS_2 -QDs as the final product (Fig. 1).

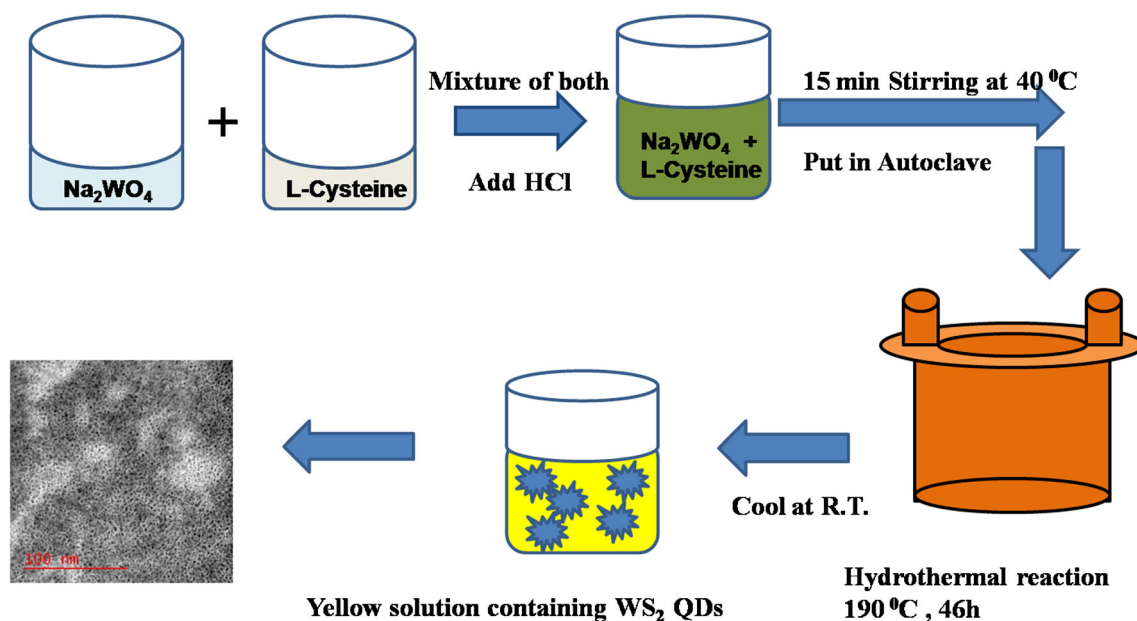


Fig. 1 Schematic representation of preparation of WS₂ QDs

Preparation of rGO

Graphene oxide (GO) was synthesized with graphite powder using well known improved Hummer's method [40] with some modification. To start with 1.5 g of graphite powder was pre-oxidized with equal amount of K₂S₂O₈, and P₂O₅ (5 g each) in 40 ml of 98% H₂SO₄ at 80 °C for 4 h. Then suspension obtained was washed for 4–5 times by deionized water (DI) kept at 50 °C in vacuum oven. In the next step, pre-oxidized graphite was further oxidised by a mixture of concentrated H₂SO₄ and H₃PO₄ in 180: 13 volume ratio under continuous stirring. 9 g of KMnO₄ was added after 5 min in the above reaction mixture. Temperature was maintained at 50 °C and the stirring was continued for 15 h. Then the reaction was stopped and left to cool down to R.T. 200 ml ice was added to reaction mixture, followed by the addition of 1.5 mL of 30% H₂O₂. A U.S. standard testing sieve (pore size 30 μm) was used to separate fine material from the mixture. Thus obtained filtrate was

centrifuged for 3 h at 5000 rpm. Sediment material was washed a number of times with DI water, HCl (30%) and ethanol and separated by centrifugation. A suspension was made in 100 mL ether with the concluding sediment and filtered by PTFE membrane (pore size = 0.45 μm).

Afterwards, to obtain rGO, the resultant suspension was sonicated for 2 h more. At R.T., hydrazine hydrate was added drop by drop in the exfoliated GO suspension in 9: 7 ratio and then reduced the mixture at 100 °C for 1 h. Resulting precipitate was filtered with cellulose filter paper and washing was done with 1 M HCl and DI until pH was 7. In the final step, filtrate was dried at R.T. for 24 h to get rGO.

Preparation of the rGO@WS₂ quantum dot composite

rGO@WS₂QDs composite is prepared by mixing both WS₂ QDs and rGO in 1:1 ratio by volume using probe sonicator for 2 h at R.T.

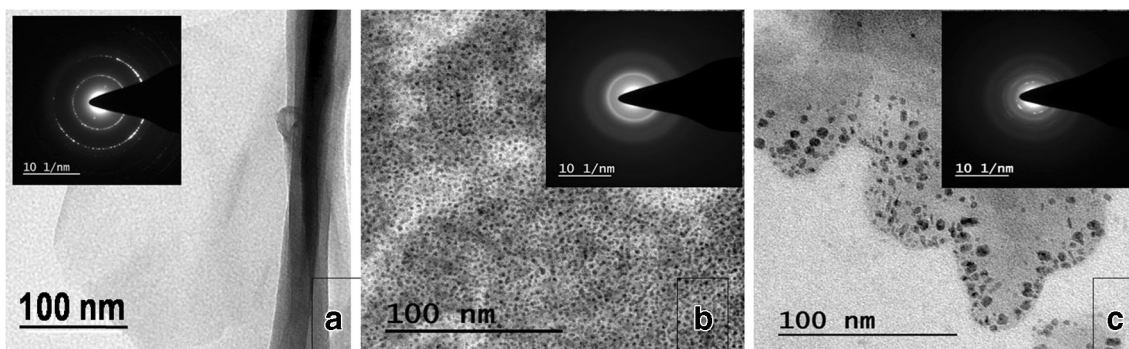


Fig. 2 Structural investigation by TEM a) rGO b) WS₂ QDs and c) rGO@WS₂ QDs (insets showing their corresponding SAED pattern)

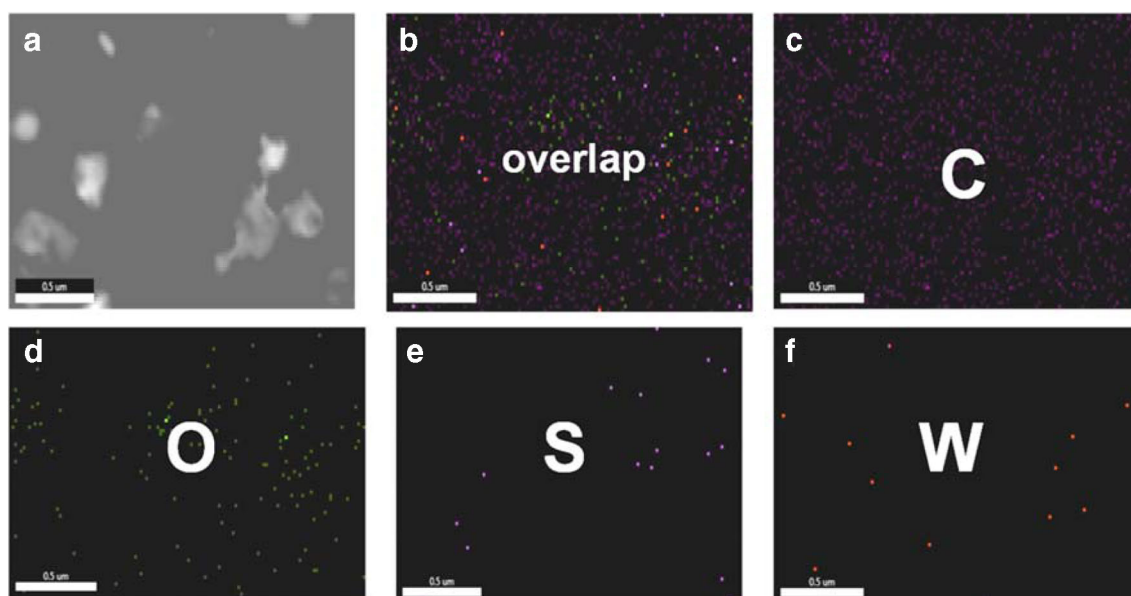


Fig. 3 EDAX mapping for rGO@WS₂ QDs (a) TEM image of information collection area, (b) overlap, (c) C element, (d) O element, (e) S element and (f) W element

Preparation of modified electrode

A glassy carbon electrode (GCE) with a geometrical surface area of 0.07 cm² was used as a substrate for the modification with rGO@WS₂ QDs nanostructures. Before modification, GCE was cleaned on a wet polishing pad with 0.05 μm alumina slurry. Then it was washed 3–4 times with DI and further sonicated in DI for 2 min for complete surface cleaning. Then, as-prepared suspension of rGO@WS₂ QDs composite was drop casted over this cleaned and polished GCE surface and allowed to dry at ambient temperature for 5–6 h and then used for all electrochemical measurements.

Results and discussions

Characterization of nanomaterials by FT-IR and UV-visible spectroscopy

The interaction between WS₂ QDs and rGO was acquired with FT-IR spectroscopy and shown in fig. S1 of ESI. FT-IR spectra were analysed for all three samples in order to justify the composite formation. The FT-IR spectra of WS₂ QDs, rGO and rGO@WS₂ QDs have been presented in the fig. S1. A broad and strong peak at 3130–3500 cm⁻¹ is attributed to the -O-H and -N-H stretching. A strong peak at 1635 cm⁻¹ is assigned to the stretching vibration of -C=O of the carboxylic group [41]. FT-IR of rGO was same as earlier works reported in literature and exhibiting different types of possible functional groups where 3435 cm⁻¹ correspond to O-H stretching vibration, 1635 cm⁻¹ showed -C=O stretching, -C=C stretching vibration at 1654 cm⁻¹, -C-OH deformation vibration at 1384 cm⁻¹ and a low intensity broad band at 1040 cm⁻¹ for -C-O(epoxide)

vibration and -C-OH vibration of -COOH groups [42]. The characteristics peaks of both WS₂ QDs and rGO are observed in the rGO@WS₂ QDs sample that elucidate the successful decoration of WS₂ QDs over rGO sheets. On comparison, the difference in the -O-H stretching vibration and the peak deviation towards longer wavelength are ascribed to the interaction among WS₂ QDs and -OH groups of rGO.

Further UV-Vis. absorption spectrum of WS₂ QDs, rGO and rGO@WS₂ QDs has been investigated and shown in fig. S2 of ESI. WS₂ QDs. showed two absorption peak at 262 nm and 364 nm which was observed because of its excitonic feature. Absorption peak of rGO was found at 265 nm which endorsed the π - π^* transition in the doubly bonded carbon atoms. Further the interaction of rGO@WS₂ QDs was observed because of the quenching of peaks at 261 nm and 326 nm [40, 43].

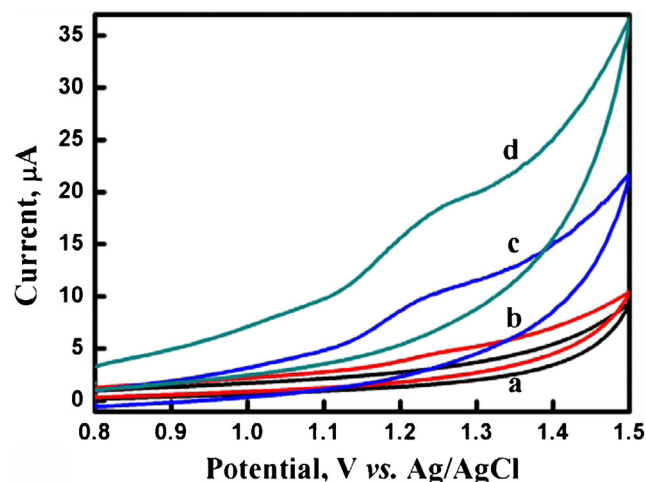


Fig. 4 Cyclic voltammetric (CV) response of different modified electrodes in phosphate buffer (pH 6) for 50 μM CQ at (a) bare GCE, (b) rGO modified GCE (c) WS₂ QDs modified GCE and (d) rGO@WS₂ QDs modified GCE

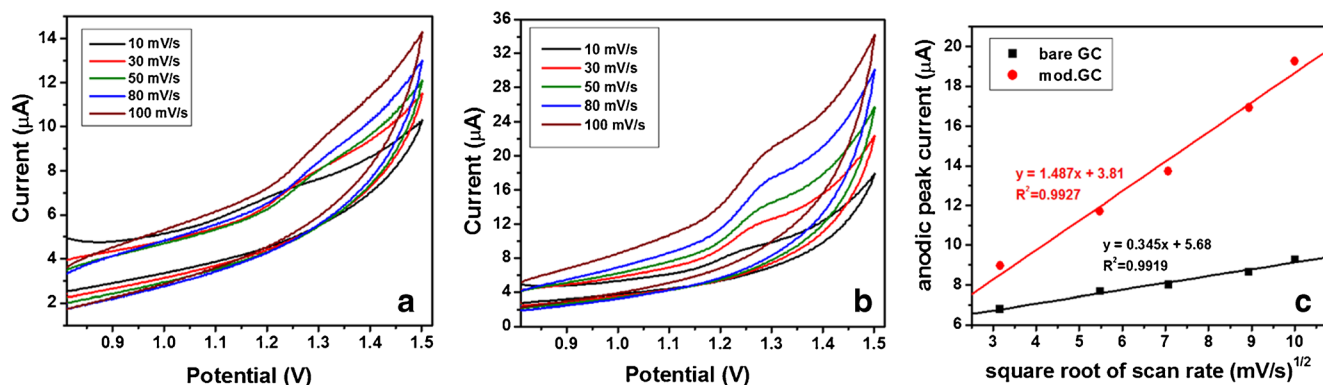


Fig. 5 CV response of (a) bare GCE and (b) rGO@WS₂ QDs modified GCE at different scan rates: 10, 30, 50, 80, 100 mV/s, in 0.1 M phosphate buffer (pH 6) in presence of 50 µM CQ (c) Plot of anodic peak potentials versus square root of scan rates for bare and rGO@WS₂ QDs modified GCE

Structural characterisation and Elemental analysis of nanomaterials by TEM, EDAX and EDAX mapping

HRTEM was used to unravel the atomic structure of rGO, WS₂ QDs and the composite. Specimens for TEM were prepared using dilute samples by drop-casting method onto the carbon-coated TEM grids and left over for complete drying for 24 h in vacuum. TEM images of rGO (Fig. 2a) reveal the sheet like morphology. Single- or few-layered nanosheets of rGO are observed with plenty of wrinkles. Intrinsic nature of graphene is recommended by corrugation and scrolling. The water soluble WS₂ QDs were characterized by TEM. The TEM image demonstrates the monodispersity of WS₂ QDs (Fig. 2b). Its structure is further verified by SAED pattern which reveals the polycrystalline nature of WS₂ QDs. Further TEM image of rGO@WS₂ QDs (Fig. 2c) reveals that the prepared composite has the signature of the quantum dots distributed over nanosheets. In addition, EDAX technique was used to investigate the presence of different elements in

rGO, WS₂ QDs and rGO@WS₂ QDs composite (Fig. S3). EDAX spectra of rGO@WS₂ QDs (Fig. S3c) display the signals for Carbon, Oxygen, Tungsten and Sulphur which prove their existence in the synthesized composite. EDAX mapping was also performed to confirm the constant distribution of all elements in rGO@WS₂ QDs composite as shown in Fig.3.

Comparative study of different modified electrode towards CQ detection

To investigate the potential application of synthesized rGO, WS₂ QDs and rGO@WS₂ QDs composite, Glassy carbon electrode was chosen and modified by different materials. Performance of different modified GCEs (WS₂ QDs modified GCE, rGO modified GCE and rGO@WS₂ QDs modified GCE) were thoroughly investigated for CQ detection by CV (Fig. 4). It is observed that in all cases CQ oxidation occurs almost at same potential but displays different current values. The highest current response is obtained in case of rGO@WS₂ QDs modified GCE as compared to WS₂ QDs modified GCE

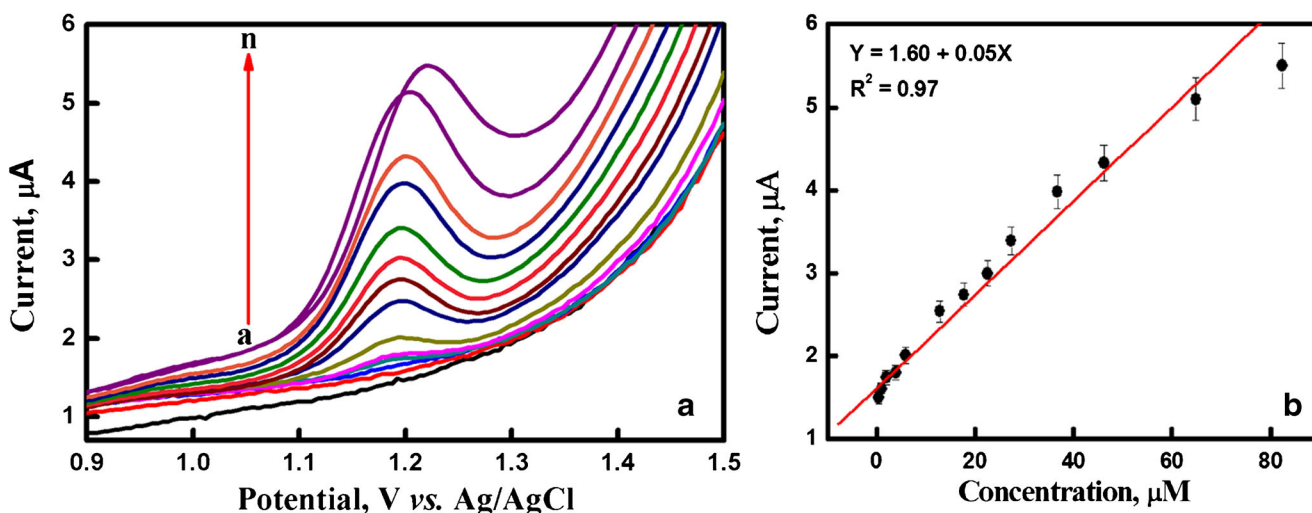


Fig. 6 DPV curve (a) and its calibration plot (b) of rGO@WS₂ QDs modified GCE in the presence of CQ (0.5 µM to 82.4 µM) in 0.1 M phosphate buffer at pH = 6

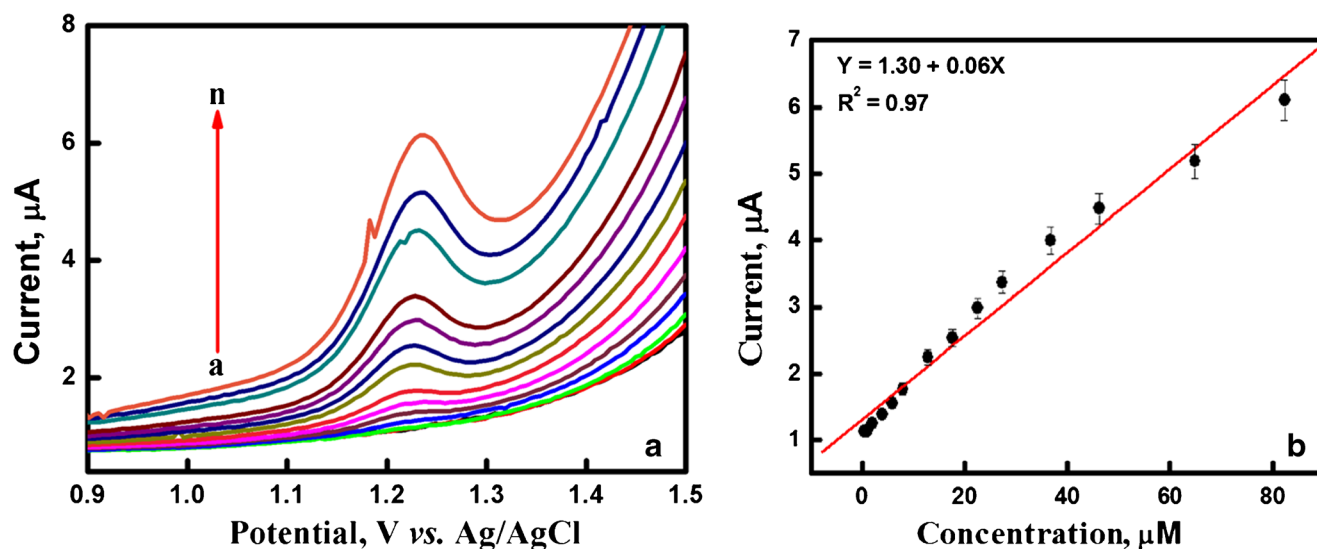


Fig. 7 DPV curve (a) and its calibration plot (b) of rGO@ WS₂ QDs modified GCE in the presence of CQ (0.5 μM to 82.4 μM in human blood serum diluted with 0.1 M phosphate buffer at pH = 6 in 1: 4 ratio)

and rGO modified GCE. This happens reasonably due to synergistic interaction between both the components.

Further CVs of Chloroquine were recorded at a series of scan rates ranging from 10 mV/s to 100 mV/s in 0.1 M phosphate buffer at bare GCE (Fig. 5a) and rGO@WS₂ QDs modified GCE (Fig. 5b). It was revealed that in both the cases, the peak current increased on increasing the scan rate. According to Randles-Sevcik equation [44].

$$i_p = (2.69 \times 10^5) n^{3/2} A C D^{1/2} \nu^{1/2} \quad (1)$$

where i_p is the anodic peak current, n is the number of exchanged electrons, A is the surface area of electrode (cm²), C is the bulk concentration (mol cm⁻³), ν is the scan rate (V/s) and D is the diffusion coefficient. From Eq. (1), current shows direct relation with the concentration as well as square root of the scan rate. Keeping the CQ concentration same, the anodic peak current i_p was plotted against the square root of different

scan rate for the bare as well as modified GCE and straight line was found in both the cases. Figure 5c shows that the anodic peak current increases linearly with the square root of the scan rate, indicating that this electrochemical process is a diffusion controlled process. The curve suggests the faster electron transfer for rGO@WS₂ QDs modified GCE as compared to bare GCE. This is attributed to nano dimensional structure that enhances the accessible interface in between the electrolytes and electrode, facilitating the electrochemical reaction over the surface of the electrode.

Electrochemical sensing of CQ by cyclic voltammetry (CV) and differential pulse voltammetry (DPV)

After optimisation of various experimental conditions, electrochemical trace level detection of chloroquine phosphate was performed via CV and DPV techniques at rGO@WS₂ QDs

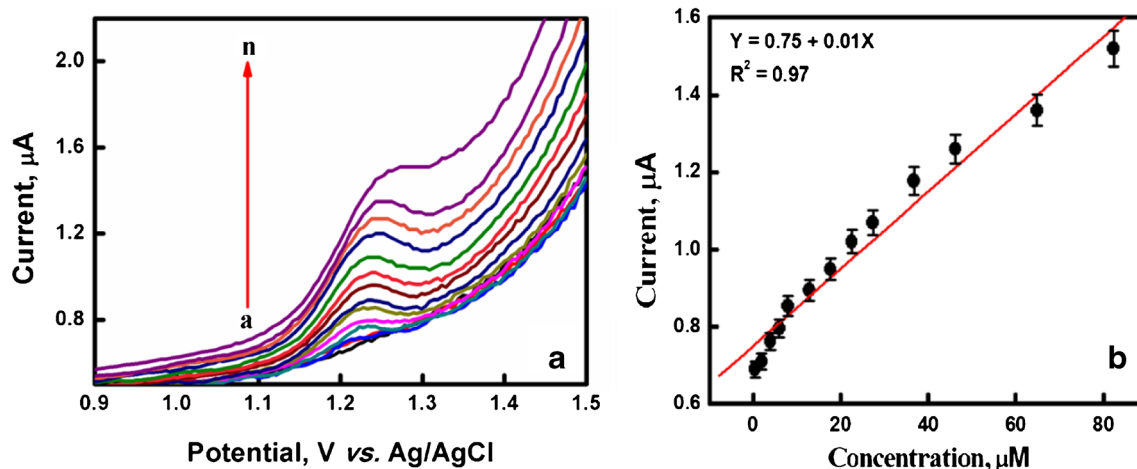


Fig. 8 DPV curve (a) and its calibration plot (b) of rGO@ WS₂ QDs modified GCE in the presence of commercially available CQ tablet (0.5 μM to 82.4 μM) in 0.1 M phosphate buffer at pH = 6

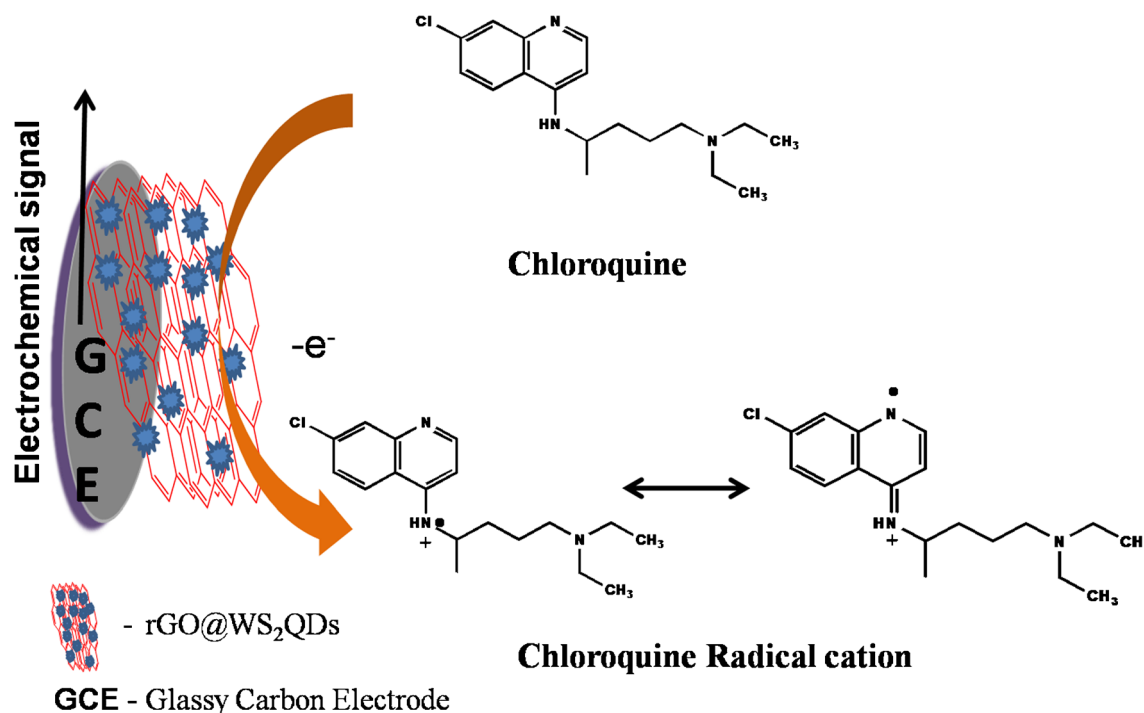


Fig. 9 Schematic representation of plausible mechanism for electrooxidation of CQ on rGO@WS₂ QDs modified GCE

composite modified nanostructured electrode in 0.1 M phosphate buffer (pH = 6). The rGO@WS₂ QDs modified GCE responds quickly towards oxidation of CQ on serial addition from 0.5 μM to 82.4 μM concentration. As the concentration of CQ increases, anodic peak current of CQ also increases gradually which is clearly depicted in its corresponding calibration plot shown with each CV and DPV plots (Fig. S4A, S4B and Fig. 6a, b). On addition of higher concentration, peak potential is shifted towards higher values which suggests that oxidation of CQ is a diffusion controlled process. Electrochemical sensing of CQ is performed in the linear range from 0.5 μM to 82.4 μM concentration with regression coefficient in the order of 0.97. The LOD and sensitivity is found to be 40 nM and 0.800 $\mu\text{A}\mu\text{M}^{-1}\text{cm}^{-2}$ respectively through DPV (Fig. 6a, b). The excellent sensitivity towards CQ detection is obtained due to larger surface area, high electroactivity and connected structures of rGO@WS₂ QDs composite through various functionalities.

After successful detection of CQ at rGO@WS₂ QDs modified GCE in 0.1 M phosphate buffer (pH 6), sensing was performed in human serum in order to investigate any major complications that might be related to test real samples by both CV and DPV (Fig. S5A, S5B and Fig. 7a, b). Blood samples of a healthy and adult person was collected and blood cells were removed through centrifugation. The obtained serum was diluted five times using phosphate buffer. After dilution, pH of buffer was checked and there was no change in pH. Same sensing behaviour is obtained at rGO@WS₂ QDs modified GCE in serum from 0.5 μM to 82.4 μM

concentration with linear calibration. The calibration plot obtained offers limit of detection (LOD) 120 nM with 0.900 $\mu\text{A}\mu\text{M}^{-1}\text{cm}^{-2}$ sensitivity at S/N: 3 (Fig. 7a, b). The same sensing behaviour in human serum also confirms the validity of proposed sensor in other biological fluids.

Chloroquine phosphate is a potent drug against malaria. So, strategy of its sensing cannot be completed before its detection in pharmaceutical formulations. For this purpose, tablets of CQ were purchased from a medical shop. A tablet of CQ was powdered using mortar and pestle and finely ground. Versatility of CQ detection was explored by acquiring same experimental parameters as employed in ideal sensing.

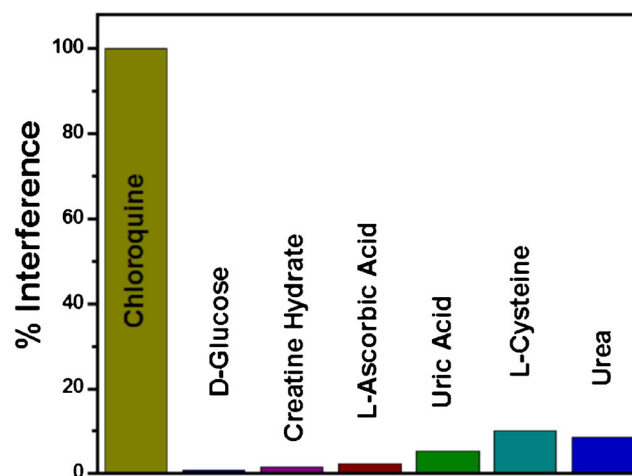


Fig. 10 Interference studies of different biological species with CQ in the ratio of 10:1 by DPV in 0.1 M phosphate buffer at pH = 6

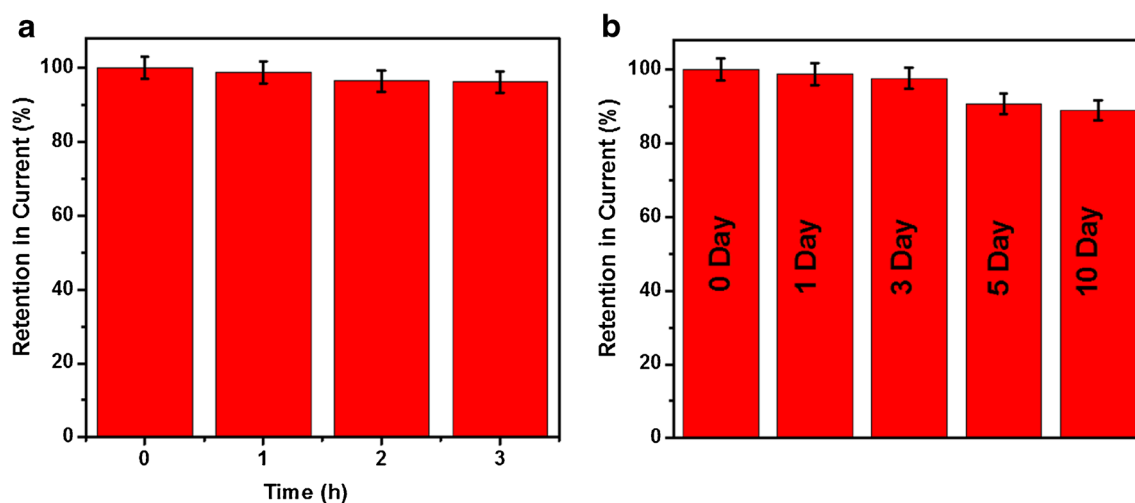


Fig. 11 **a** Intra-day study and **(b)** Inter-day study of developed electrochemical sensor by DPV in 0.1 M phosphate buffer at pH = 6 in presence of 50 μM CQ

Same voltammetric response was obtained at rGO@WS₂ QDs modified GCE on successive addition of tablet solution with linear calibration range of 0.5 μM to 82.4 μM concentration in both CV and DPV (Fig. S6A, S6B and Fig. 8a, b). The obtained calibration plot offers good LOD as 80 nM and sensitivity of 0.143 $\mu\text{A}\mu\text{M}^{-1}\text{cm}^{-2}$ at S/N: 3 by DPV (Fig. 8a, b).

As seen from both CV and DPV curves, Chloroquine is oxidized in 1.20 V - 1.25 V potential range, which was shown in the form of oxidation peak. It is found that this oxidation process was irreversible, as no cathodic peak was found in CV. A plausible electro-sensing mechanism for Chloroquine involves its electro-oxidation over rGO@WS₂ QDs modified GCE as shown in Fig. 9. The synthesized material may probably augment the conductivity of electrode and facilitate the process of electron transfer, thereby improving the analytical selectivity and sensitivity towards the detection of the particular analyte. Also, high electro-catalytic efficiency of rGO@WS₂ QDs facilitates a superior corridor for electro-oxidation performance of chloroquine [40]. Thus anodic peak shown in each DPV or CV may be ascribed to the irreversible oxidation of the *N*-heterocyclic nitrogen of the aminoquinoline moiety and the nitrogen of alkylamino side chain grouping of chloroquine molecule [12, 45, 46].

Interference study

It is well known that human blood serum has many other biocomponents viz. carbohydrates, amino acids, lipids, salts etc., which can interfere in desired drug detection and hinder the selectivity of proposed electrochemical sensor or biosensor. Thus, we have performed experiments with some common molecules present in human blood serum. Results described in Fig. 10, for D-glucose, Creatine hydrate, L-ascorbic acid, uric acid, L-cysteine and urea, showed very less or negligible interference even at 10 times higher concentration of each interferent (500 μl of 1 mM stock) with respect to concentration of chloroquine (50 μl of 1 mM stock).

Reproducibility and stability study

Developed sensor can be used 2–3 times due to less change in current values as shown in Fig. 11a. For a particular concentration of drug it is observed that developed sensor showed retention of current upto 97%. After 3 h of time interval, only 2–3% current is decreased which shows that our developed sensor shows reliable stability or can be reused. On the other hand interday stability investigation of developed sensor shows that it is adequately stable upto 10 days. More than

Table 1 Comparative study for electrochemical detection of Chloroquine based on earlier reported works

Modified Electrode	Technique	Supporting electrolyte	LOD μM	Linear Range μM	Matrix	Ref.
dsDNA/CPE	CV/DPV	B-R/ PB	0.03	0.1–10	Spiked human serum	[12]
CuNW/CPE	DPV	PB	0.02	0.13–13.3	Pharmaceutical formulation	[47]
rGO@WS ₂ /GCE	CV	PB	0.04	0.5 - 82.4	Human blood serum & Pharmaceutical formulation	Present work
	DPV	PB	0.04	0.5 - 82.4	Human blood serum & Pharmaceutical formulation	

LOD, Lower Detection limit; dsDNA, double stranded DNA; CuNW, Cu(OH)₂Nanowire; CPE, Carbon paste electrode; GCE, Glassy carbon electrode; CV, Cyclic voltammetry; DPV, Differential pulse voltammetry; PB, Phosphate buffer

90% current is retained as displayed in Fig. 11b. The electrode is highly stable towards CQ sensing and can be applied for many days with good accuracy.

Our developed sensor is highly sensitive towards detection of CQ in buffer, real samples and in pharmaceutical formulations without any interference. The electrode shows reliable stability and it can be compared with other developed sensors reported earlier in literature in Table 1.

Conclusions

We developed a sensitive 2D composite-modified GCE for electrochemical detection of anti malarial drug, Chloroquine phosphate by two techniques, CV and DPV simultaneously. The composite serves as a nano-mediator for the rapid transfer of electron to the electrode from the redox centre. The rGO@WS₂ QDs modified GCE is highly sensitive towards detection of CQ from 0.5 μM to 82.4 μM concentration range with 40 nM limit of detection (LOD) at signal to noise ratio (S/N): 3. Detection of CQ is also performed in real samples (human serum) as well as in pharmaceutical formulations. Our developed sensing platform is highly sensitive and reliable for developing electro-sensing devices using screen printed electrodes and open new avenues in the field of electro-sensing.

Acknowledgements The first author (MS) is grateful to DST, New Delhi (SR/WOS-A/CS-52/2018) for fellowship. The authors are also thankful to Prof. D. Dash, Institute of Medical Science, BHU, Varanasi, for the help extended towards availing blood serum and CIF, IIT (BHU) Varanasi for providing various characterization facilities.

Compliance with ethical standards The author(s) declare that they have no competing interests. Monika Srivastava and Preeti Tiwari with Vineet have carried out experiments and are responsible for raw data if required. Human blood serum was collected from blood donors of the institute using our institute hospital (Institute of Medical Sciences, BHU, Varanasi) facility following the methods in accordance with relevant guidelines and regulations. All experimental protocols were approved by the Biochemistry lab of the Institute of Medical Sciences, BHU, Varanasi and further, it is sanctioned by institutional committee (Institute Ethical Committee) and consent was obtained from all subjects.

References

1. Tracy JW, Webster LT, Brunton L, Parker K, Lazo J, Buxton I (1996) Goodman and Gilman's the pharmacological basis of therapeutics, D. Blumenthal (Eds.), McGraw-Hill, New York, , pp. 965
2. Weingarten HL, Cherry EJA (1981) A chloroquine fatality. *Clin Toxicol* 18:959–963. <https://doi.org/10.3109/15563658108990324>
3. Thapliyal N, Chiwunze TE, Karpoomath R, Goyal RN, Patel H, Cherukupalli S (2016) Reasearch progress in electroanalytical techniques for detremination of antimalarial drugs in pharmaceutical and biological samples. *RSC Adv* 6:57580–57680. <https://doi.org/10.1039/c6ra05025e>
4. Saad B, Zin ZM, Jab MS, Rehman IA, Saleh MI, Mahsufi S (2005)Flow-through chloroquine sensor and its applications in pharmaceutical analysis. *Anal Sci* 21:521–524. <https://doi.org/10.2116/analsci.21.521>
5. Savarino A, Trani LD, Donatelli I, Cauda R, Cassone A (2006) New insights into the antiviral effects of chloroquine. *Lancet Infect Dis* 6:67–69. [https://doi.org/10.1016/S1473-3099\(06\)70361-9](https://doi.org/10.1016/S1473-3099(06)70361-9)
6. Sotelo J, Briceño E, López-González MA (2006) Adding chloroquine to conventional treatment for *Glibostoma Multifforme*: a randomized, double-blind, placebo-controlled trial. *Ann Intern Med* 144:337–343. <https://doi.org/10.7326/003-4819-144-5-200603070-00008>
7. Muhm M, Stimpfl T, Malzer R, Mortinger H, Binder R, Vycudilik W, Berzlanovich A, Bauer G, Laggner AN (1996) Suicidal chloroquine poisoning: clinical course, autopsy findings, and chemical analysis. *J Forensic Sci* 41:1077–1079. <https://doi.org/10.1520/JFS14054J>
8. Qarah ASN, Basavaiah K, Swamy N (2017) Sensitive and selective extraction-free spectrophotometric assay of chloroquine phosphate in pharmaceuticals based on ion-pair reaction with Bromocresol green and Bromocresol purple. *Pharm Anal Acta* 8(3):539–566. <https://doi.org/10.4172/2153-2435.1000539>
9. Ducharme J, Farinotti R (1997) Rapid and simple method to determine chloroquine and its desethylated metabolites in human microsomes by high-performance liquid chromatography with fluorescence detection. *J Chromatogr B* 698:243–250. [https://doi.org/10.1016/S0378-4347\(97\)00273-9](https://doi.org/10.1016/S0378-4347(97)00273-9)
10. Croes K, McCarthy PT, Flanagan RJ (1994) Simple and rapid HPLC of quinine, Hydrochloroquine, chloroquine, and Desethylchloroquine in serum, whole blood, and filter paper-adsorbed dry blood. *J Anal Toxicol* 18:255–260. <https://doi.org/10.1093/jat/18.5.255>
11. Papadopoulos K, Triantis T, Dimotikali D, Nikokavouras J (2000)Radiostorage- and photostoragechemiluminescence: analytical prospects. *Anal Chim Acta* 423:239–245. [https://doi.org/10.1016/S0003-2670\(00\)01118-1](https://doi.org/10.1016/S0003-2670(00)01118-1)
12. Radi A (2005) Accumulation and trace measurement of chloroquine drug at DNA-modified carbon paste electrode. *Talanta* 65: 271–275. <https://doi.org/10.1016/j.talanta.2004.05.024>
13. Jiao L, Zhang L, Wang X, Diankov G, Dai H (2009) Narrow graphene nanoribbons from carbon nanotubes. *Nature* 458:877–880. <https://doi.org/10.1038/nature07919>
14. Park S, Ruoff RS (2009) Chemical methods for the production of graphenes. *Nat Nanotechnol* 4:217–224. <https://doi.org/10.1038/nnano.2009.581>
15. Ding J, Sun W, Wei G, Su Z (2015) Cuprous oxide microspheres on graphene nanosheets: an enhanced material for non- enzymatic electrochemical detection of H₂O₂ and glucose. *RSC Adv* 5: 35338–35345. <https://doi.org/10.1039/C5RA04164C>
16. Zhang P, Lu X, Huang Y, Deng J, Zhang L, Ding F, Su Z, Wei G, Schmidt OG (2015) MoS₂ nanosheets decorated with gold nanoparticles for rechargeable LiO₂ batteries. *J Mater Chem A* 3:14562–14566. <https://doi.org/10.1039/C5TA02945G>
17. Zhu S, Wang J, Fan W (2015)Graphene-based catalysis for biomass conversion. *Catal Sci Technol* 5:3845–3858. <https://doi.org/10.1039/C5CY00339C>
18. Kim KS, Zhao Y, Jang H, Lee SY, Kim JM, Kim KS, Ahn J-H, Kim P, Choi J-Y, Hong H (2009) Large scale pattern growth of graphene films for stretchable transparent electrodes. *Nature* 457:706–710. <https://doi.org/10.1038/nature07719>
19. Neto AHC, Guinea F, Peres NMR, Novoselov KS, Geim AK (2009) The electronic properties of graphene. *Rev Mod Phys* 81: 109–162. <https://doi.org/10.1103/RevModPhys.81.109>
20. Liu Z, Liu Q, Huang Y, Ma Y, Yin S, Zhang X, Sun W, Chen Y (2008) Organic photovoltaic devices based on a novel acceptor material: graphene. *Adv Mater* 20:3924–3930. <https://doi.org/10.1002/adma.200800366>

21. Xiong D, Li X, Shan H, Zhao Y, Dong L, Xu H, Zhang X, Li D, Sun X (2015) Oxygencontaining functional groups enhancing electrochemical performance of porous reduced graphene oxide cathode in lithium ion batteries. *Electrochim Acta* 174:762–769. <https://doi.org/10.1016/j.electacta.2015.06.041>
22. Beceril HA, Mao J, Liu Z, Stoltenberg RM, Bao Z, Chen Y (2008) Evaluation of solution processed reduced graphene oxide films as transparent conductors. *ACS Nano* 2:463–470. <https://doi.org/10.1021/nn700375n>
23. Shin H-J, Kim KK, Benayad A, Yoon S-M, Park HK, Jung I-S, Jin MH, Jeong H-K, Kim JM, Choi J-Y, Lee YH (2009) Efficient reduction of graphite oxide by sodium borohydride and its effect on electrical conductance. *Adv Funct Mater* 19:1987–1992. <https://doi.org/10.1002/adfm.200900167>
24. Yin S, Men X, Sun H, She P, Zhang W, Wu C, Qin W, Chen X (2015) Enhanced photocurrent generation of bio-inspired graphene/ZnO compsite films. *J Mater Chem A* 3:12016–12022. <https://doi.org/10.1039/C5TA02297E>
25. Du Y, Zhao Y, Qu Y, Chen CH, Chen CM, Chuang CH, Zhu Y (2014) Enhanced light-matter interaction of graphene-gold nanoparticle hybrid films for high performance SERS detection. *J Mater Chem C* 2:4683–4691. <https://doi.org/10.1039/C4TC00353E>
26. Zhao X, Zhang P, Chen Y, Su Z, Wei G (2015) Recent advances in the fabrication and structure-specific applications of graphene-based inorganic hybrid membranes. *Nanoscale* 7:5080–5093. <https://doi.org/10.1039/C5NR00084J>
27. Kumar A, Prakash R (2014) Graphene sheets modified with Polyindole for electrochemical detection of dopamine. *J Nanosci Nanotechnol* 14:2501–2506. <https://doi.org/10.1166/jnn.2014.8549>
28. Salavagione HJ, Díez-Pascual AM, Lázaro E, Vera S, Gómez-Fatou MA (2014) Chemical sensors based on polymer composites with carbon nanotubes and graphene: the role of the polymer. *J Mater Chem A* 2:14289–14328. <https://doi.org/10.1039/C4TA02159B>
29. Liu Y, Wang R, Zhu Y, Li R, Zhang J (2015) Photochemical sensing of catechol based on CdS-DNA-pristine graphene nanocomposite film. *Sensors Actuators B Chem* 210:355–361. <https://doi.org/10.1016/j.snb.2014.12.124>
30. Srivastava M, Nirala NR, Srivastava SK, Prakash R (2018) A comparative study of Aptasensor vs Immunosensor for label-free PSA Cancer detection on GQDs-AuNRs modified screen-printed electrodes. *Sci Rep* 8:1923–1933. <https://doi.org/10.1038/s41598-018-19733-z>
31. Chen M, Su H, Mao L, Guo M, Tang J (2018) Highly sensitive electrochemical DNA sensor based on the use of three-dimensional nitrogen-doped graphene. *Microchim Acta* 185:51–59. <https://doi.org/10.1007/s00604-017-2588-2>
32. Xing L, Ma Z (2016) A glassy carbon electrode modified with nanocomposite consisting of MoS₂ and reduced graphene oxide for electrochemical simultaneous determination of ascorbic acid, dopamine, and uric acid. *Microchim Acta* 183:257–263. <https://doi.org/10.1007/s00604-015-1648-8>
33. Dadkhah S, Ziaei E, Mehdinia A, Kayyal TB, Jabbari A (2016) A glassy carbon electrode modified with amino-functionalized graphene oxide and molecularly imprinted polymer for electrochemical sensing of bisphenol a. *Microchim Acta* 183:1933–1941. <https://doi.org/10.1007/s00604-016-1824-5>
34. Yan X, Dai Y, Chen M, Wang J, Ren J, Wang Q, Wu Y, Ye N, Wang Y, Cheng X (2017) WS₂ nanosheets decorated by ag nanoparticles with different content and uniform distribution for enhanced electrochemical properties. *J Nanopart Res* 19(5):165–173. <https://doi.org/10.1007/s11051-017-3865-z>
35. Zhang XH, Tan H, Fan Z, Ge MZ, Ye X, Xue MQ (2017) Synthesis and electrochemical performance of ultrathin WS₂ nanosheets. *Chalcogenide Lett* 14(10):419–423
36. Zhou Y, Sui C, Yin H, Wang Y, Wang M, Ai S (2018) Tungsten disulfide (WS₂) nanosheet-based photoelectrochemical aptasensing of chloramphenicol. *Microchim Acta* 185(10):453–460. <https://doi.org/10.1007/s00604-018-2970-8>
37. Gopalakrishnan D, Damien D, Shaijumon MM (2014) MoS₂ Quantum dot-interspersed exfoliated MoS₂ Nanosheets. *ACS Nano* 8:5297–5303. <https://doi.org/10.1021/nn501479e>
38. Yang Z-C, Wang M, Yong AM, Wong SY, Zhang X-H, Tan H, Chang AY, Li X, Wang J (2011) Intrinsically fluorescent carbon dots with tunable emission derived from hydrothermal treatment of glucose in the presence of monopotassium phosphate. *Chem Commun* 47:11615–11617. <https://doi.org/10.1039/C1CC14860E>
39. Yang Y, Cui J, Zheng M, Hu C, Tan S, Xiao Y, Yang Q, Liu Y (2012) One-step synthesis of amino-functionalized fluorescent carbon nanoparticles by hydrothermal carbonization of chitosan. *Chem Commun* 48:380–382. <https://doi.org/10.1039/C1CC15678K>
40. Tiwari P, Nirala NR, Prakash R (2018) Determination of the anti-HIV drug Nevirapine using electroactive 2D material Pd@rGO decorated with MoS₂ quantum dots. *Chemistry Select* 3:5341–5347. <https://doi.org/10.1002/slct.201702250>
41. Zhao X, He D, Wang Y, Fu C (2018) Facile fabrication of tungsten disulfide quantum dots (WS₂ QDs) as effective probes for fluorescence detection of dopamine (DA). *Mater Chem Phys* 207:130–134. <https://doi.org/10.1016/j.matchemphys.2017.12.045>
42. Singh MK, Pandey RK, Prakash R (2017) High-performance photo detector based on hydrothermally grown SnO₂ nanowire/reduced graphene oxide (rGO) hybrid material. *Org Electron* 50:359–366. <https://doi.org/10.1016/j.orgel.2017.08.016>
43. Yan Y, Zhang C, Gu W, Ding C, Li X, Xian Y (2016) Facile synthesis of water-soluble WS₂ quantum dots for turn-on fluorescent measurement of lipoic acid. *J Phys Chem C* 120:12170–12177. <https://doi.org/10.1021/acs.jpcc.6b01868>
44. Rafati AA, Afriz A (2014) Amperometric sensing of anti-HIV drug zidovudine on ag nanofilm-multiwalled carbon nanotubes modified glassy carbon electrode. *Mater Sci Eng C* 39:105–112. <https://doi.org/10.1016/j.msec.2014.02.037>
45. Mathur NC, Goyal RN, Malik WU (1990) Oxidation of 2-aminoquinoline at a stationary pyrolytic graphite electrode. *Anal Chim Acta* 230:91–93. [https://doi.org/10.1016/S0003-2670\(00\)82765-8](https://doi.org/10.1016/S0003-2670(00)82765-8)
46. Lama K, Stephen J, Van W, William EG (2017) One-electron oxidation of chloroquine, cymanquine, and related aminoquinolines in nonaqueous media. *J Electroanal Chem* 799:531–537. <https://doi.org/10.1016/j.jelechem.2017.06.041>
47. Mashhadizadeh MH, Akbarian M (2009) Voltammetric determination of some anti-malarial drugs using a carbon paste electrode modified with Cu(OH)₂ nano-wire. *Talanta* 78:1440–1445. <https://doi.org/10.1016/j.talanta.2009.02.040>

Publisher's note Springer Nature remains neutral with regard to jurisdictional claims in published maps and institutional affiliations.